Chemical Engineering Journal 379 (2020) 122323

Contents lists available at ScienceDirect

Chemical Engineering Journal

journal homepage: www.elsevier.com/locate/cej

A novel and green method to synthesize a epoxidized biomass eucommia gum as the nanofiller in the epoxy composite coating with excellent anticorrosive performance

Bo Chen[a], Qian Wu[a], Ji Li[a], Kaidong Lin[a], Dongchu Chen[c], Chengliang Zhou[a], Tao Wu[a], Xiaohu Luo[a,b,*], Yali Liu[a,*]

[a] State Key Laboratory for Chemo/Biosensing and Chemometrics, College of Chemistry and Chemical Engineering, Hunan University, Changsha, Hunan 410082, PR China
[b] School of Chemistry and Chemical Engineering, Qiannan Normal University for Nationalities, Duyun 558000, PR China
[c] School of Material Science and Energy Engineering, Foshan University, Foshan 528000, PR China

HIGHLIGHTS

- Epoxidized biomass eucommia gum (EEUG) was successfully synthesized by an interfacial reaction.
- EEUG/epoxy composite coatings with 1 wt% showed an improvement in the tensile strength.
- EEUG/epoxy composite coatings with 1 wt% exhibited the outstanding anticorrosion protection performance.

GRAPHICAL ABSTRACT

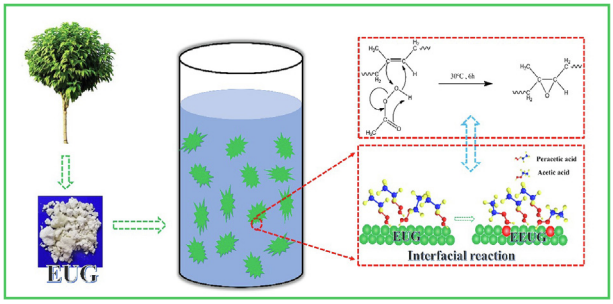

ARTICLE INFO

Keywords:
Eucommia gum
Interfacial reaction
Corrosion resistance
Epoxy coating

ABSTRACT

The design and preparation of a long term effective anticorrosion coating in a large scale in the harsh environment is still an enormous challenge for the anticorrosion technology. Herein, Eucommia gum, a natural biomass rubber material, had been epoxidized by a novel and green method involved in an interfacial reaction using the water as a dispersant. Epoxidized biomass eucommia gum (EEUG) is utilized as a functional filler in the synthesis of epoxy composite coating. The epoxy groups in the EEUG can react with the hardener, not only resulting in the event dispersion of EEUG in the composite coating, but also leading to the formation of the much richer crosslinking densities. A substantial improvement in the corrosion protection and the tensile strength were obtained. For example, EEUG/epoxy composite coatings with 1 wt% EEUG still maintains excellent anticorrosion performance with the high polarization resistance (R_f) values of $8.846 \times 10^8\ \Omega\,cm^2$ after 30 days of immersion times in the harsh environment (3.5 wt% NaCl solution, pH = 7). The implication of the present study for utilization of the natural biomass rubber material to enhance the physical and mechanical properties of polymeric matrixes has been discussed, and a great anticorrosion coating is provided.

* Corresponding authors at: State Key Laboratory for Chemo/Biosensing and Chemometrics, College of Chemistry and Chemical Engineering, Hunan University, Changsha, Hunan 410082, PR China (X. Luo and Y. Liu).
E-mail addresses: luoxiaohu4812350@163.com (X. Luo), yaliliu@hnu.edu.cn (Y. Liu).

https://doi.org/10.1016/j.cej.2019.122323
Received 7 May 2019; Received in revised form 19 July 2019; Accepted 23 July 2019
Available online 24 July 2019
1385-8947/

1. Introduction

Steel as a constructing material has been widely application in all the world [1–5]. However, the steels in these structures are prone to corrosion, especially in the marine environment containing many corrosive media, such as chloride, water, oxygen, and so on [6–8]. Material failure due to corrosion often causes great harm to human lives and properties every year. Therefore, it is imperative to develop an effective strategy to prevent the steel from corrosion. Nowadays, there are many anti-corrosion methods, including metal surface modification, corrosion inhibitors, and organic protection coatings [9–14]. Organic coatings have some fascinating advantages, such as high efficiency, convenience, and low-cost [15]. Epoxy coating, as an organic coating, shows excellent mechanical properties, acid and alkali resistance, wear resistance and insulation [16–21]. Also, it can be seen as a good anticorrosive coating [16]. However, the epoxy resin as a coating material has two obvious drawbacks. On the one hand, there are some inevitable solvents, and the volatilization of these solvents often causes some micro-pores in the epoxy coating during the curing process. On the other hand, there always are some voids among polymer chains. The two defects allow corrosive mediums in the environment to contact the metal substrate, causing the occurrence of the corrosion on the surface of metal [22]. Thereby, solving the two defects plays an important role in the further application.

Addition of impermeable nanofillers (i.e., carbon back, clay, carbon nanotubes, and graphene) has been a common and efficient way to solve the defects [13,15,22–28]. Currently, Graphene is considered as the most anticipated barrier filler, exhibiting excellent corrosion resistance [29–38]. However, due to its electrical conductivity, it can accelerate the corrosion of the metal substrate, resulting in the material failure [39–43]. Similarly, rubber shows good corrosion protection property due to its outstanding barrier effect. Compared with graphene, rubber has non-conducting characteristics and has been a great potential application in the anticorrosion materials. For example, Hossein Yahyaei et al. [44] added an epoxy-terminated poly-butadiene rubber into the epoxy resin to obtain an effective corrosion-resistant and wear-resistant epoxy coating with good toughening and hydrophobic effects. However, to our best knowledge, there have been few researches on the addition of renewable natural rubber into the epoxy coatings to enhance the corrosion protection. Furthermore, on the one hand, the compatibility between natural rubber and epoxy resin is poor due to the difference in the polarity. On the other hand, the rubber is not well dispersed because of its two large molecular weight. There are various approaches to improve the compatibility between natural rubber and epoxy resin, such as the addition of solubilizers, the chemical modification of polymers, co-solvent method, and manufacturing interpenetrating network structure (IPN) method [45–48].

Eucommia gum (EUG) with the molecular weight in the range of 120,000–300,000 is a natural biomass rubber extracted from the bark and leaves of Eucommia ulmoides. As a special functional polymer material, EUG is excellent in fatigue resistance, abrasion resistance, shock resistance, and tear resistance, and it has other excellent properties, such as easy crystallization, low melting point, strong insulation, water resistance, acid and alkali resistance, and chlorine ion resistance [49–52]. At present, some reports demonstrated that the epoxidation modification has a great improvement on the compatibility of EUG with high polarity materials [53]. Despite this, a lot of organic solvents were used during the procedure of epoxidation reaction, such as toluene, chloroform, and petroleum ether, which causes environmental issues [53]. Therefore, it is necessary to develop a green method to modify the EUG for the improvement of the compatibility.

Based on the above analyses, in this work, epoxidized biomass eucommia gum (EEUG) has been successfully synthesized through a novel and green method involved in the interfacial reaction using the water as the dispersant. As-obtained EEUG as a nanofiller shows the enhanced compatibility with epoxy coating. The degree of the epoxidation for EEUG was characterized by Fourier transform infrared spectroscopy (FT-IR), and the epoxy value was determined by the chemical titration. The compatibility of the EEUG with the epoxy coating and the distribution in the coating were observed by scanning electron microscopy (SEM). Simultaneously, the glass transition temperature and the thermal properties of the EEUG was determined by the differential scanning calorimetry (DSC) and the thermo-gravimetry, respectively. Additionally, the tensile measurements were carried out to determine the effect of the addition of EEUG on the mechanical properties of the epoxy composite coating. Interestingly, a series of electrochemical measurements show that the corrosion protection performance of epoxy composite coating is greatly improved due to the good dispersion of EEUG in the composite coating. It is believed that the EEUG has great potential application in the anticorrosive field, and our work has also developed a new strategy for other rubber applications.

2. Experimental

2.1. Raw materials

Concentrated hydrochloric acid, sodium hydroxide, H_2O_2 (30%wt), glacial acetic acid (CH_3COOH), butyl Alcohol ($C_4H_{10}O$) and xylene were purchased from China National Pharmaceutical Group Co. Epoxy resin (E51), polyamide hardener (Ancamide351A), antifoaming agent (Byk-085), leveling agent (Deqian-839), and dispersing agent (Deqian-9850) were purchased from Zhuzhou Feilu High-tech Materials Co., Ltd. (China). Eucommia ulmoides Gum (EUG) was purchased from Xiangxi Laojiao Biological Co., Ltd. (China). The mild steel panels and Tinplate were purchased from Hunan Xiangjiang Kansai Paint Co., Ltd. (China). Deionized water (Self-made).

2.2. Preparation of epoxidized eucommia ulmoides gum (EEUG)

In this work, the EEUG is synthesized through a facile and green method, which is shown in Fig. 1. Firstly, eucommia ulmoides gum (5 g) was cut into the small particles, then were transferred to a three-necked 100 mL round-bottom flask equipped with a magnetic stirrer, and the water (50 mL) was added. After that, the mixer was heated to 30 °C, and a mixed of H_2O_2 (4.5 g) and glacial acetic acid (2.82 g) must be slowly dropped in 6 h under the magnetic stirring. Subsequently, the production was washed with deionized water for several times until pH = 7.0, and then kept it in an oven for 12 h at 75 °C for the evaporation of water. Finally, it was dried in a vacuum oven at 50 °C for 12 h.

2.3. Preparation of EEUG/epoxy resin composite coating

The mixture of butyl alcohol and xylene (V_1:V_2 = 7:3) was used to dissolve the mentioned above EEUG at 40 °C for half an hour. Epoxy resin and the EEUG were put in a 100 mL three-necked round-bottom flask equipped with a magnetic stirrer, in which the mass proportion of EEUG was 1 wt%. After 1 h stirring, the hardener was added into the flask as epoxy resin/hardener equal 2/1 (w/w). The final mixture was coated on a PTFE substrate by a glass rod. After curing at 60 °C for 24 h, the EEGU/epoxy composite coating was obtained, which was called as EEGU/epoxy composite coating with 1 wt%. The composite coating was peeled from the PTFE substrate, revealing a coating thickness of 40 mm, which was used for the mechanical and thermal properties.

For comparison, the different mass proportions of EEUG (0 wt%, 0.5 wt% and 2 wt%) were used to prepare the epoxy/EEUG composite coatings according to the above procedure, which was donated as neat epoxy coating, EEGU/epoxy composite coating with 0.5 wt%, and EEGU/epoxy composite coating with 2 wt%, respectively.

2.4. Preparation of the samples for corrosion protection performance

The mixture of butyl alcohol and xylene (V_1:V_2 = 7:3) was used to

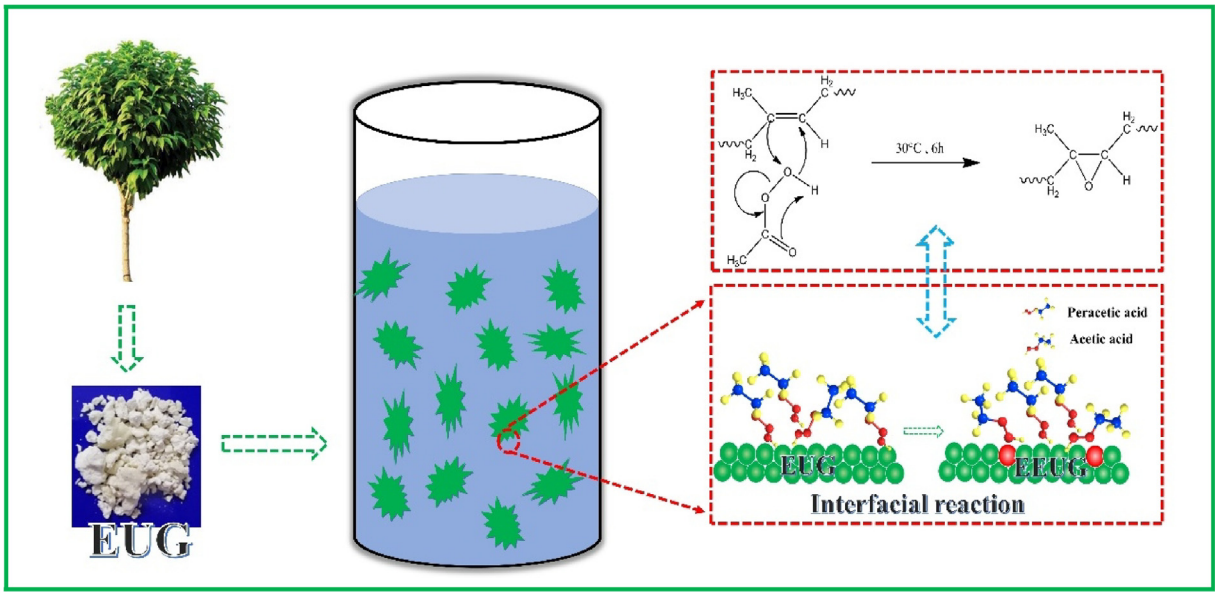

Fig. 1. Schematic representation of the synthesis of EEUG.

dissolve the mentioned above EEUG at 40 °C for half an hour. Epoxy resin and the EEUG were put in a 100 mL three-necked round-bottom flask equipped with a magnetic stirrer, in which the mass proportion of EEUG was 1 wt%. After 1 h stirring, the hardener was added into the flask as epoxy resin/hardener equal 2/1 (w/w). A steel electrode with an area of 1 cm^2 was polished, and cleaned. The mixture was coated on the surface of Q235 steel electrode by a glass rod. After curing at 60 °C for 24 h, the EEGU/epoxy composite coating with a thickness of 40.7 ± 0.2 μm was obtained. The prepared specimen was used as the working electrode for electrochemical corrosion studies.

The electrochemical impedance spectroscopy (EIS) measurements were carried out in a 3.5 wt% NaCl solution through a three-electrode system, where the coated electrode was used as the working electrode, the platinum electrode was used as a counter electrode, and the saturated calomel electrode (SCE) was used as the reference electrode. Before each EIS measurement, the open circuit potential (OCP) should reach a steady status. The EIS measurements were performed in the frequency range of 0.01 Hz–10,000 Hz. The disturbance voltage was 50 mV. The electrochemical impedance results were simulated according to suitable electrical equivalent circuits through ZSimpWin software.

2.5. Neutral salt spray test

The neutral salt spray test was conducted according to GB/T1771-91 [54]. Specimens were placed in a commercial salt-spray chamber at 35 °C. The chamber was filled with 5 wt% NaCl solution in which the pH was about 6.5, and the amount of spray should be (1–2.5) mL/h per 80 cm^2 area. Digital images of specimens were taken as recorded regularly after cleaning by the filter paper.

2.6. Thermal performance analysis

In order to analyze the thermal performance of the coating, a thermal analyzer was used to investigate the thermal stability and glass transition temperature (T_g) of the coating under a nitrogen atmosphere. The test was performed at a rate of 10 °C min^{-1} from 25 °C to 600 °C using German Benz thermogravimetric-differential thermal scanning TG-DSC (STA449C, Netzsch, Germany). DSC was performed at a rate of 10 °C min^{-1} from 25 °C to 200 °C using German Benz differential thermal scanning (Netzsch, Germany, DSC404F1 Pegasus).

2.7. Mechanical tests of the coating

Tensile test was conducted according to ASTM D638 [55]. Pencil hardness of coatings was tested as GB/T6739-1996 [56]. Adhesion test and the impact resistance were performed as GB/T9286-1998 [56] and GB/T1732-1993 [56], respectively. Chemical resistance tests were carried out at room temperature and referred to the method of Chaudhari [57].

3. Results and discussion

3.1. Characterization of EEUG

Eucommia ulmoides gum is a *trans*-polyisoprene and has the rubber and plastic duality. Because of the difference in polarity between the EUG and epoxy resin, the compatibility of the EUG with the epoxy resin is poor as shown in Fig. S1. Thus, to address the issue, a great potential method is to modify the EUG by epoxidizing the C=C in the EUG. In this work, the EEUG is synthesized through a facile and green method involved in the interfacial reaction, which is shown in Fig. 1. With the assistance of glacial acetic acid and hydrogen peroxide, the C=C in EUG is epoxidized to obtain EEUG. Fig. 2 shows the FT-IR spectra of the EEUG, EUG, and the neat epoxy resin. As seen in FT-IR spectra, the functional groups are identified. The characteristic peaks at 840 cm^{-1}, 795 cm^{-1}, 746 cm^{-1} are assigned to the in-plane bending of C–H in R_2C=CHR, resulting from the EUG [58].The characteristic peaks at 1460 cm^{-1} and 1380 cm^{-1} are attributed to the bending vibration of the methyl group, indicating that EUG and EEUG both have the methyl groups. The peak at 1665 cm^{-1} owns to the stretching vibration of C=C. Compared with EUG, the relative intensity of C=C peaks for EEUG is obviously weakened, suggesting that the C=C is reacted. Although the relative intensity of peaks at 2940 cm^{-1} and 2840 cm^{-1} owing to the stretching vibration of the hydrocarbon decreases, the characteristic peaks still exist, indicative of the presence of C=C in the EEUG. Additionally, the peak at 3140 cm^{-1} is the stretching vibration of the C–H from epoxy resin. Interestingly, as for the EEUG, there are two new peaks appearing at 1250 cm^{-1} and 910 cm^{-1} compared to the EUG, which are attributed to the characteristic peaks of epoxy resin. Thus, it can be reasonable to confirm that the epoxidation for EUG has occurred through the interfacial reaction. Moreover, the epoxy value for the EEUG has been determined by the chemical titration. The results show that the epoxy value for the EEUG is about 0.15. Also, the

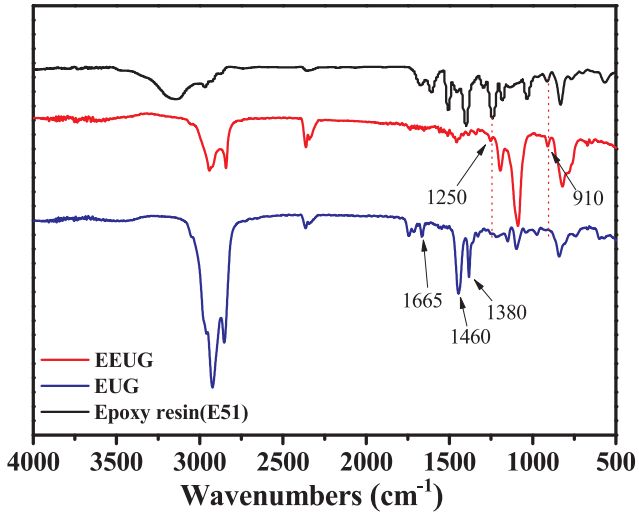

Fig. 2. FT-IR spectra of EEUG, EUG, and epoxy resin.

stretching vibration peak of the carbon-oxygen bond of alcohol locating at 1090 cm^{-1} is observed, which reveals the presence of a side reaction of epoxy ring opening.

The ^{1}H spectra of EUG and EEUG obtained by using Bruker model DRX-400 NMR spectrometer with TMS as an internal standard are shown in Fig. S2. It can be seen from Fig. S2 that the signal at 3.4 ppm is attributed to the hydrogen linked to epoxy group from the EEUG, Meanwhile, other signals from the EEUG is an agreement with EUG [59].

The obtained results show that the EEUG is successfully synthesized and the substantial structure of the EUG is retained. As expected, The EEUG exhibits the excellent compatibility with the epoxy resin as seen from Fig. S3. The EEUG was well dispersed in the epoxy resin under the vigorous stirring and ultrasonication (Fig. S3a). The dispersion is very stable and no precipitates occur after storing for 60 days (Fig. S3b).

3.2. Surface morphology of EEUG/epoxy composite coatings

To further confirm the compatibility of EEUG with epoxy resin, the surface and cross-sectional morphologies of the composite coatings with different contents of EEUG and neat epoxy coating were characterized by SEM. Fig. 3 displays the SEM images of the surface of neat epoxy coating and EEUG/epoxy composite coatings. It can be seen in Fig. 3a that the surface of the epoxy resin is smooth. The composite coatings containing the 0.5 wt% and 1 wt% EEUG (Fig. 3b–c) are also as smooth as epoxy resin. However, when the doped contents od EEUG further increase, the surface of the composite coating (Fig. 3d) shows some white spots compared to the composite coatings containing the 0.5 wt% and 1 wt% EEUG, which may be due to the particles of free EEUG. The results also suggest that the EEUG show the good compatibility with epoxy resin when the content of EEUG in the composite coating is less than 2 wt%. Furthermore, Fig. 4 shows the cross-sectional SEM images of the neat epoxy coating and the composite coatings. As seen in Fig. 4a, the cross-section of the neat epoxy resin is smooth, but has some with river-like cracks, which may result from the crack growth, and the bubble-like circle is a dispersant. Compared to the neat epoxy coating, the composite coatings containing the 0.5 wt% and 1 wt % EEUG (Fig. 4b–c) has less river-like cracks and are more smooth. This indicates that the compatibility of the epoxy resin with the EEUG is

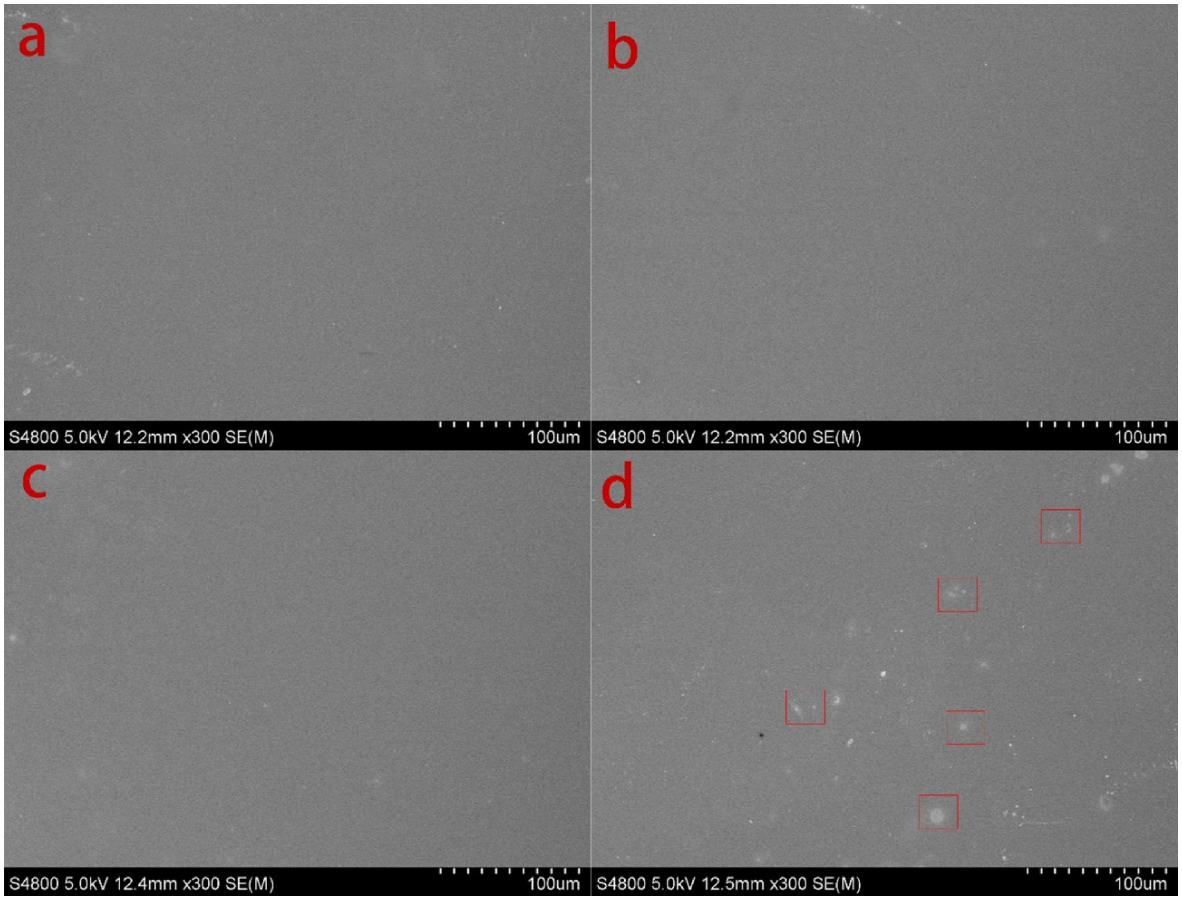

Fig. 3. SEM images of (a) neat epoxy coating, (b) EEUG/epoxy composite coating with 0.5 wt%, (c) EEUG/epoxy composite coating with 1 wt%, and (d) EEUG/epoxy composite coating with 2 wt%.

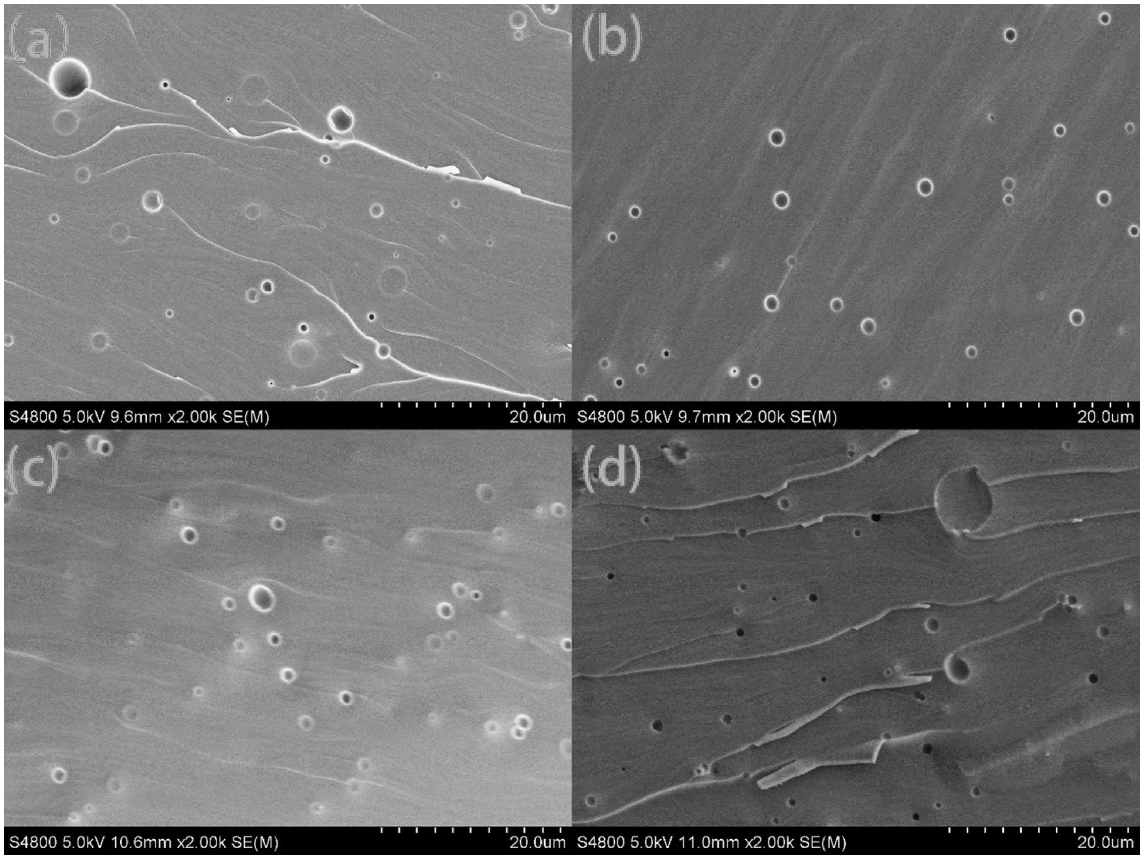

Fig. 4. Cross-sectional SEM images of (a) neat epoxy coating, (b) EEUG/epoxy composite coating with 0.5 wt%, (c) EEUG/epoxy composite coating with 1 wt%, and (d) EEUG/epoxy composite coating with 2 wt%.

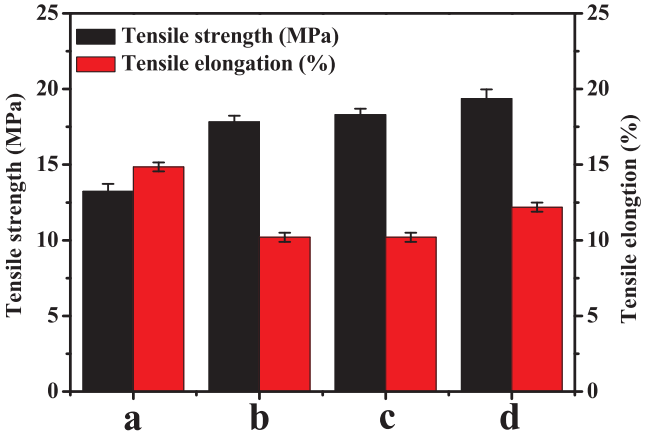

Fig. 5. Tensile strength and elongation of (a) neat epoxy coating, (b) EEUG/epoxy composite coating with 0.5 wt%, (c) EEUG/epoxy composite coating with 1 wt%, and (d) EEUG/epoxy composite coating with 2 wt%.

obviously enhanced. However, in the case of the composite coatings with 2 wt% EEUG (Fig. 4d), the cross section has some recessed sections, which may be produced by the reuniting of free EEUG. As the above-obtained results, it is considerable to reveal that when the doped contents of EEUG are 0.5 wt% and 1 wt%, the EEUG can be well dispersed in the EEUG/epoxy composite coatings. Nevertheless, with a further increase of the doped EEUG in the composite coating, the macromolecular EEUG can be reunited to form the large particles (i.e., free EEUG), leading to the poor compatibility of EEUG with epoxy.

3.3. Mechanical properties of the EEUG/epoxy composite coatings

To understand the effect of EEUG on the mechanical properties of the composite coatings, the tensile measurements were carried out. The obtained results are exhibited in Fig. 5. In the case of the neat epoxy coating, the tensile strength value is about 13.23 Mpa. As for the composite coatings with different doped contents of EEUG, the tensile strength increases with the doped contents of EEUG, reaches 18.03 MPa, which is larger than that of the neat epoxy coating. This suggests that the introduction of EEUG enhances the tensile strength of the composite coating compared to the neat epoxy coating. This

Table 1
The other mechanical properties of the coatings.

Coatings	Appearance	Pencil hardness	Adhesion	Wet adhesion	Impact resistance	Chemical resistance	
						Acid (5%H_2SO_4), 48 h	Alkali (5%NaOH), 48 h
Neat epoxy resin	Smooth	4H	0	0	50 cm	Corrosion	Swell
EEUG/epoxy composite coating with 0.5 wt%	Smooth	4H	0	0	50 cm	Pass	Pass
EEUG/epoxy composite coating with 1 wt%	Smooth	4H	1	1	48 cm	Pass	Pass
EEUG/epoxy composite coating with 2 wt%	Smooth	4H	2	2	48 cm	Pass	Pass

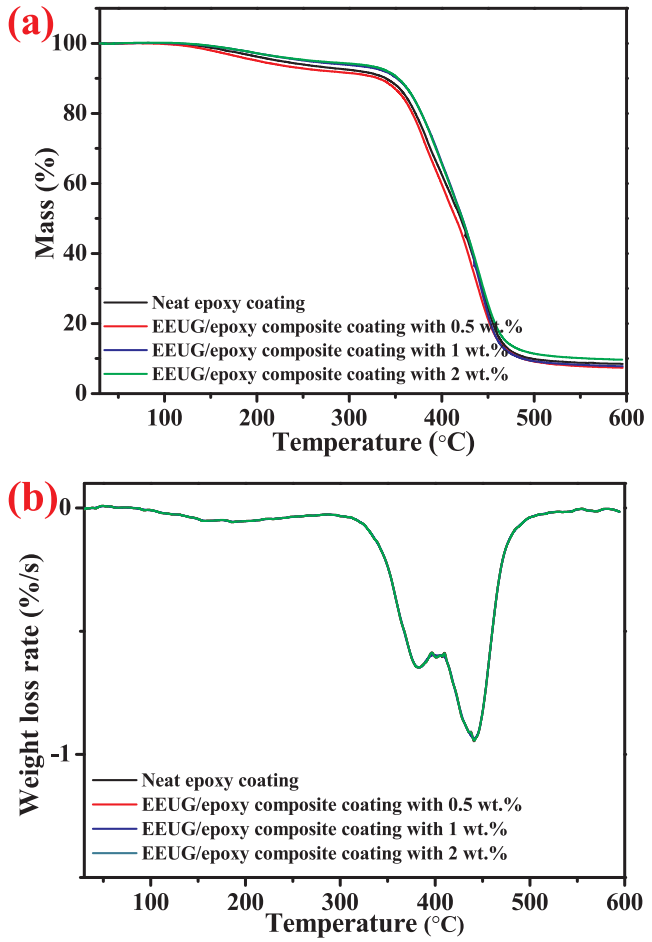

Fig. 6. (a) TGA analysis and (b) the derived curves of neat epoxy coating, EEUG/epoxy composite coating with 0.5 wt% EEUG, EEUG/epoxy composite coating with 1 wt% EEUG, and EEUG/epoxy composite coating with 2 wt% EEUG.

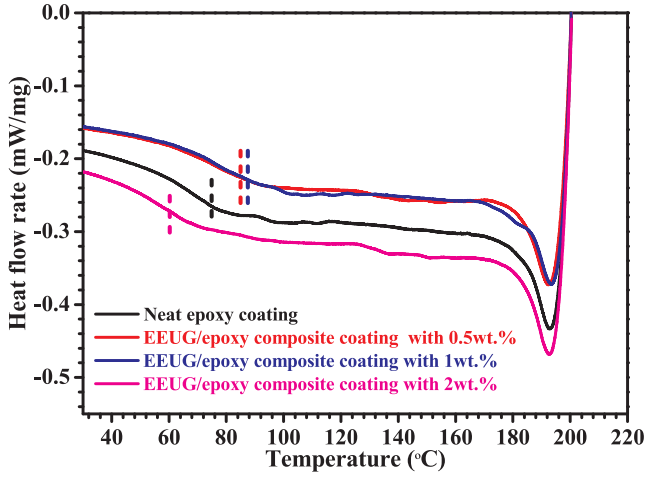

Fig. 7. DSC curves of neat epoxy coating, EEUG/epoxy composite coating with 0.5 wt% EEUG, EEUG/epoxy composite coating with 1 wt% EEUG, and EEUG/epoxy composite coating with 2 wt% EEUG.

phenomenon can be explained by that the following reasons: on the one hand, the epoxy groups in the EEUG can react with the polyamide hardener through the addition reaction during the curing process, resulting in forming the closer interpenetrating network structures. On the other hand, EEUG has the larger relative molecular mass and the

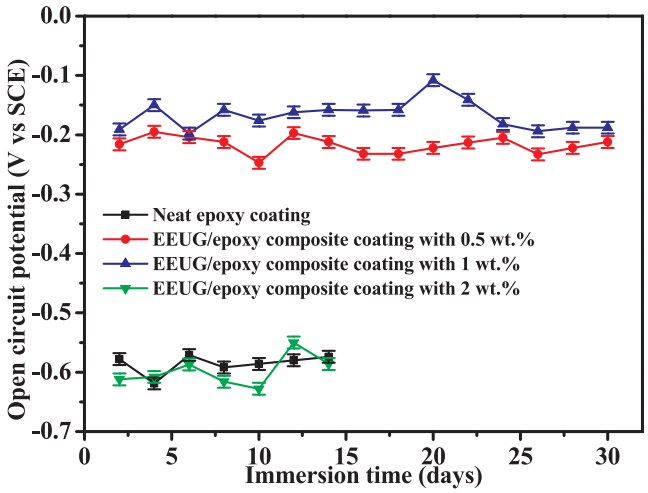

Fig. 8. The changes of open circuit potential of neat epoxy coating, EEUG/epoxy composite coating with 0.5 wt%, EEUG/epoxy composite coating with 1 wt%, and EEUG/epoxy composite coating with 2 wt%.

long molecular chain, so it is easier to entangle with the epoxy resin owing to the rapid evaporation of the solvents during the curing process, which leads to forming the denser molecular chains. Thus, the EEUG/epoxy composite coatings exhibit the richer crosslinking densities.

On the contrary, the elongation at break for the neat epoxy is greater than the composite coatings. This result indicates that the toughening for the EEUG/epoxy composite coatings decreases compared to the neat epoxy coating. This is opposite to the recently reported results [60,61]. These recently reported that the introduction of the rubber in the coating could improve the toughening due to that rubber particles could absorb energy and prevent crack growth. However, in our case, the EEUG/epoxy composite coatings have the richer crosslinking densities compared with the neat epoxy coating, so the composite coatings have the weaker toughening. Similarly, the slight increase in the elongation at break for the composite coatings with the doped contents of EEUG, which suggests that the composite coating with the 2 wt% EEUG shows the strongest toughening. This is attributed to that free EEUG (Fig. 4) appearing in the composite coatings can enhance the toughening of coating, which is consistent with the recently reported results [62].

Table 1 shows the other mechanical properties of the coatings. All the samples display the good performances of the acid-alkaline resistant and the impact resistance. For example, the acid and alkali resistance for the coatings are up to 120 h and 96 h, respectively. The composite coatings and neat epoxy coating show a similar pencil hardness. However, with the increase of EEUG, the adhesion of the composite coatings reduces. The EUG has a large molecular weight and the content of epoxy group is relatively low, so the adsorption with the substrate is relatively poor, which reduces the adhesion of the coating.

3.4. Thermal stability of the EEUG/epoxy composite coatings

Fig. 6 reveals the TGA curves of the EEUG/epoxy composite coatings and neat epoxy coating. It is noteworthy that the decomposition profiles of the EEUG/epoxy composite coatings and neat epoxy coatings show the similar decomposition profiles with degradation occurring in two stages. Seeing from Fig. 6a, the weight loss doesn't occur when the temperature is below 120 °C, which means that all coatings do not contain the water and solvent. The small loss occurring between 120 °C and 380 °C should be ascribed to the pyrolysis of the antifoaming agent, leveling agent, and dispersing agent. In Fig. 6b, two decomposition peaks appear in 380 °C–485 °C, indicating that all the sample has two decomposition process. This suggests the degradation of epoxy resin

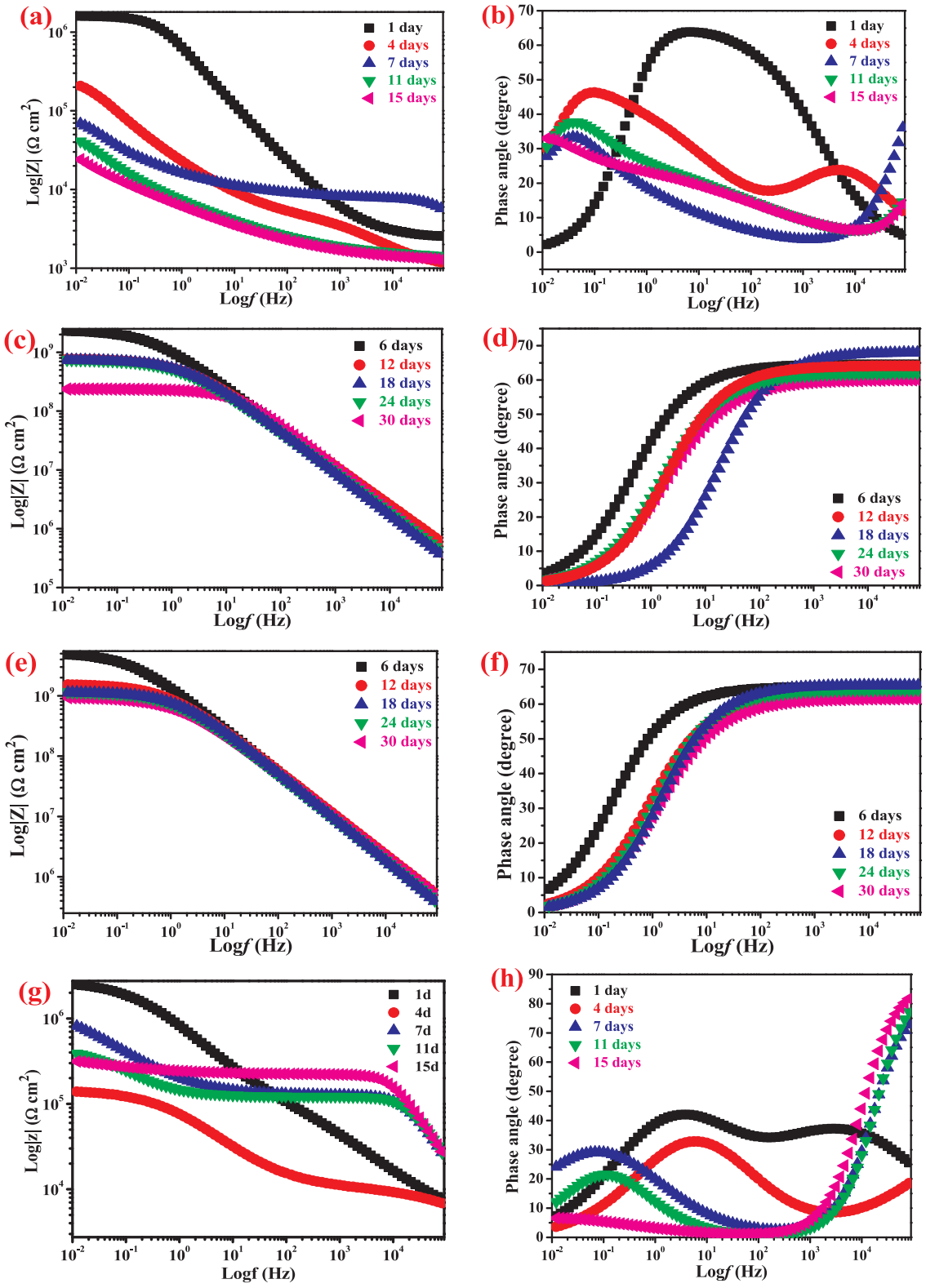

Fig. 9. Time-depended Bode and phase angle plots of (a, b) neat epoxy coating, (c, d) EEUG/epoxy composite coating with 0.5 wt%, (e, f) EEUG/epoxy composite coating with 1 wt%, and (g, h) EEUG/epoxy composite coating with 2 wt%.

follows a complicated mechanism [63]. The results suggest that the introduction of EEUG doesn't compromise the thermal properties of epoxy. Moreover, to determine the influence of the EEUG on glass transition temperature (T_g) of the coating, differential thermal scanning (DSC) was conducted. Fig. 7 shows the DSC curves of the EEUG/epoxy composite coatings and neat epoxy coating. It is clearly seen from Fig. 7 that the EEUG/epoxy composite coating with 1 wt% has the highest T_g values, which is approximately 82.84 °C. The EEUG/epoxy composite coating with 1 wt% has the lowest T_g because of the increase in free volume fractions in the polymer coatings [64].

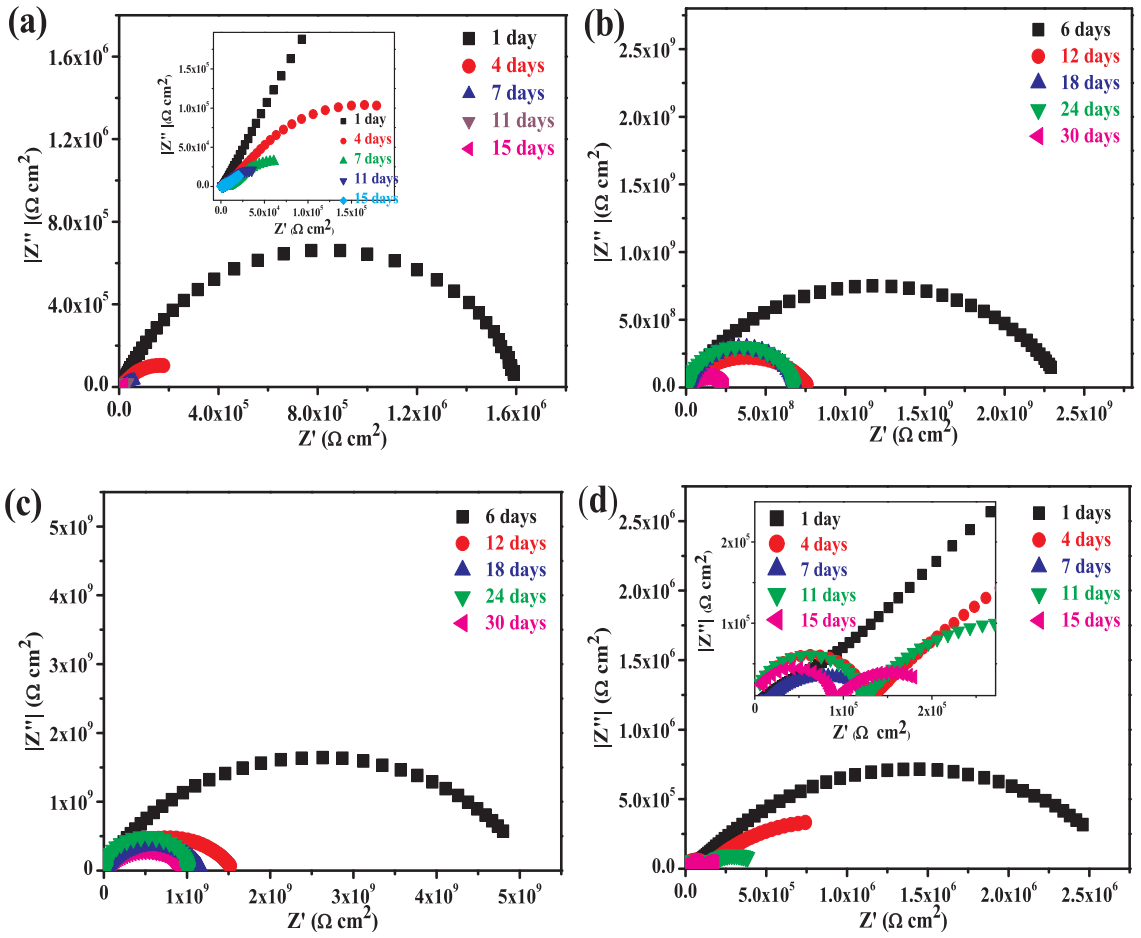

Fig. 10. Time-depended Nyquist diagrams of (a) neat epoxy coating, (b) EEUG/epoxy composite coating with 0.5 wt%, (c) EEUG/epoxy composite coating with 1 wt %, and (d) EEUG/epoxy composite coating with 2 wt%.

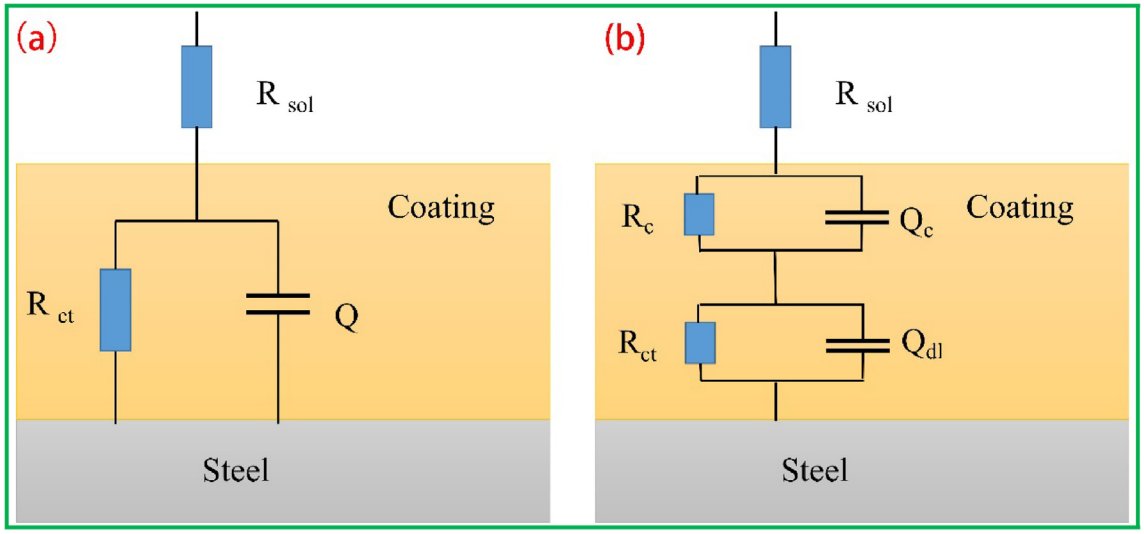

Fig. 11. The equivalent electrical circuits employed to simulate the impedance data of the samples.

3.5. Corrosion resistance of the EEUG/epoxy composite coatings

Open circuit potential ($E_{(OCP)}$) was performed to quantitatively analyze the corrosion resistance of the composite coatings with the different contents of EEUG and the neat epoxy coating in 3.5 wt% NaCl solution at pH = 7 for different immersion times. The obtained results are shown in Fig. 8. As for the EEUG/epoxy composite coating with 1 wt %, the $E_{(OCP)}$ value is the largest among the all coatings during the immersion times, stabilizing at larger than −0.2 V/SCE during the 30 days of the immersion times. The $E_{(OCP)}$ value for the EEUG/epoxy composite coating with 0.5 wt% EEUG stabilizes at slightly lower than −0.2 V/SCE during the immersion times. However, the neat epoxy coating and the EEUG/epoxy composite coating with 2 wt% has the lower $E_{(OCP)}$ during the 15 days of the immersion times, keeping at

Table 2
The electrochemical impedance parameters fitted from the measured impedance data in Fig. 9.

Coating	Immersion times (days)	R_c (Ω cm^2)	Q_c		C_c (F/cm^2)	R_{ct} (Ω cm^2)	Q_{dl}		C_{dl} (F/cm^2)	R_f (Ω cm^2)
			Y ($\Omega^{-1}cm^{-2}S^n$)	n			Y ($\Omega^{-1}cm^{-2}S^n$)	n		
Neat epoxy coating	1	1.804×10^6	3.331×10^{-7}	0.7543	2.82×10^{-7}					1.804×10^6
	4	5.450×10^5	1.583×10^{-5}	0.5934	6.93×10^{-5}	4.556×10^3	2.577×10^{-6}	0.5193	4.21×10^{-8}	5.496×10^5
	7	7.959×10^3	1.193×10^{-5}	0.8642	8.24×10^{-6}	2.786×10^4	4.979×10^{-5}	0.4211	7.81×10^{-5}	3.582×10^4
	11	2.610×10^3	1.032×10^{-4}	0.2943	4.42×10^{-6}	3.492×10^4	2.858×10^{-4}	0.8154	4.81×10^{-4}	3.753×10^4
	15	2.150×10^3	7.801×10^{-4}	0.6323	1.05×10^{-3}	3.699×10^4	1.263×10^{-4}	0.2881	5.69×10^{-3}	3.914×10^4
EEUG/epoxy composite coating with 0.5 wt%	6	2.376×10^9	1.988×10^{-10}	0.7171	1.47×10^{-10}					2.376×10^9
	12	7.732×10^8	2.497×10^{-10}	0.6672	1.09×10^{-10}					7.732×10^8
	18	6.446×10^8	6.065×10^{-10}	0.8132	3.79×10^{-10}					6.446×10^8
	24	6.017×10^8	7.665×10^{-10}	0.8711	5.13×10^{-10}					6.017×10^8
	30	3.321×10^8	1.102×10^{-9}	0.6234	1.03×10^{-9}					3.321×10^8
EEUG/epoxy composite coating with 1 wt%	6	5.151×10^9	1.741×10^{-10}	0.7222	1.67×10^{-10}					5.151×10^9
	12	1.556×10^9	1.956×10^{-10}	0.6963	1.16×10^{-10}					1.556×10^9
	18	1.114×10^9	3.517×10^{-10}	0.7138	3.51×10^{-10}					1.114×10^9
	24	9.815×10^8	8.118×10^{-9}	0.8725	6.18×10^{-9}					9.815×10^8
	30	8.846×10^8	9.912×10^{-9}	0.9145	1.01×10^{-8}					8.846×10^8
EEUG/epoxy composite coating with 2 wt%	1	4.063×10^6	4.514×10^{-7}	0.4616	6.24×10^{-8}					4.063×10^6
	4	2.056×10^6	6.465×10^{-7}	0.6505	1.15×10^{-7}	1.167×10^6	5.082×10^{-6}	0.6719	2.15×10^{-6}	3.223×10^5
	7	1.242×10^5	4.094×10^{-6}	0.4256	3.02×10^{-5}	1.157×10^5	7.340×10^{-11}	0.9898	7.34×10^{-11}	2.399×10^5
	11	1.217×10^5	7.146×10^{-6}	0.6713	1.12×10^{-5}	1.216×10^5	7.019×10^{-11}	0.9885	7.02×10^{-11}	2.433×10^5
	15	8.930×10^4	2.497×10^{-5}	0.7037	3.50×10^{-5}	1.265×10^5	7.324×10^{-11}	0.9936	7.06×10^{-11}	2.158×10^5

around −0.6 V/SCE. This means that the corrosion resistance of the EEUG/epoxy composite coatings with 0.5 and 1 wt% EEUG is significantly enhanced compared to the neat epoxy coating, owing to the presence of EEUG in the composite coatings.

To further determine the corrosion protection properties of the coatings, the electrochemical impedance spectroscopy (EIS) measurements were carried out. The time-depended Bode, phase diagrams and Nyquist diagrams of the EEUG/epoxy composite coatings and neat epoxy coatings are shown in Figs. 9 and 10, respectively. Especially, the immersion times for the neat epoxy coating and the composite coating with 2 wt% are 15 days, since the coatings on the steel electrode surface have dropped and the steels have been seriously corroded. The others are 30 days. It is seen from Fig. 9a–d that the impedance modulus values at 0.01 Hz ($|Z|_{0.01Hz}$) of the neat epoxy coating and the composite coating with 2 wt% EEUG are greater than $10^6\ \Omega\,cm^2$ after 1 day of the immersed time. Meanwhile, they have only one maximum phase angle. This means it can represent a typical behavior of the initial organic coating soaking [65]. The coatings can be realized as a good barrier to prevent the metal substrate from the corrosion. After 4 days immersed in 3.5 wt% NaCl solution, a new time constant appears in Fig. 9b, meanwhile, the impedance modulus at 0.01 Hz ($|Z|_{0.01Hz}$) significantly decreases. This indicates that the corrosive medium has passed through the coating and is in contact with the metal substrate, leading to the occurrence of the corrosion on the metal surface. With further increase in the immersed times, the $|Z|_{0.01Hz}$ of neat epoxy coating evidently drops. After 15 days of immersion times, the $|Z|_{0.01Hz}$ values is less than $10^5\ \Omega\,cm^2$, which means that the corrosion protection for the neat epoxy coating has failed. As for the composite coating with 2 wt%, after 4 days of immersion times, the $|Z|_{0.01Hz}$ suddenly increases (Fig. 9g). This is explained by that the metal substrate is corroded by the electrolyte presented at the surface of metal and forms a protective oxide film. However, the immersion times are expanded to 15 days, the corrosive mediums passed through the protective oxide film and continued to corrode the metal substrate, which is evidenced by the remarkable decrease of the $|Z|_{0.01Hz}$ (less than $10^5\ \Omega\,cm^2$) and phase angle (Fig. 9g–h). In the case of the composite coating with 0.5 and 1 wt% EEUG, after 30 days of the immersion times, the $|Z|_{0.01Hz}$ values are about $3.74 \times 10^8\ \Omega\,cm^2$ and $9.06 \times 10^8\ \Omega\,cm^2$ (Fig. 9c and e), respectively. Moreover, the phase angles with a one-time phase during the entire immersion times (Fig. 9d and f) are in line with the typical organic coating immersion behavior [15]. These results distinctly suggest that the corrosion resistances of the EEUG/epoxy composite coatings with 0.5 and 1 wt% are significantly improved compared with the blank coating and the EEUG/epoxy composite coatings with 2 wt% EEUG.

The EIS were further analyzed by the equivalent electrical circuits as shown in Fig. 11. Fig. 11a was to fit the EIS with one time constant and the EIS with two-time constants was fitted by Fig. 11b. Q is a constant phase angle element, representing the equivalent capacitance of the coating capacitance and the electric double layer capacitance of the electrode and solution [65]. The constant-phase element is related to an equivalent capacitance such as the coating capacitance (C_c), and the capacitance of the double-charge layer (C_{dl}) can be determined by the following equation [65]:

$$C_x = (Q_x \times R_x^{1-n})^{\frac{1}{n}}$$

where the C_x, Q_x, R_x and n are the capacitance, constant-phase element, the charge transfer resistance of coating (R_c), and the empirical exponent, respectively. The fitting impedance parameters for the coatings immersed in 3.5 wt% NaCl solution at pH = 7 against the immersion duration are summarized in Table 2. Generally, when n is equal to 1, Q acts as a purely capacitive element. The polarization resistance (R_f) is often utilized to refer to the degree of difficulty for corrosion to occur on the specimen. In general, the R_f is equivalent to the sum of charge transfer resistance (R_{ct}) and coating resistance (R_p), i.e., $R_f = R_{ct} + R_c$. Commonly, the higher the R_f value is, the better the corrosion protection is. After 7 days of the immersion times, the R_f of neat epoxy coating is only $3.582 \times 10^4\ \Omega\,cm^2$, meaning that the corrosion resistance of the epoxy coating is failure, which is good agreement with the results from the Bode plots (Fig. 9a). R_f value of the EEUG/epoxy composite coating with 2 wt% decreases from $4.063 \times 10^6\ \Omega\,cm^2$ to $2.158 \times 10^5\ \Omega\,cm^2$ after 15 days of immersion times in 3.5 wt% NaCl solution, suggesting the EEUG/epoxy composite coating with 2 wt% has been seriously damaged and cannot protect the metal from corrosion. It is evident from Table 2 that the R_f of the EEUG/epoxy composite coating with 0.5 and 1 wt% is much larger than that of the EEUG/epoxy composite coating with 2 wt% and the neat epoxy coating through the immersion duration. For example, after 30 days of immersion times, the R_f values of the EEUG/epoxy composite coating with 0.5 and 1 wt% are

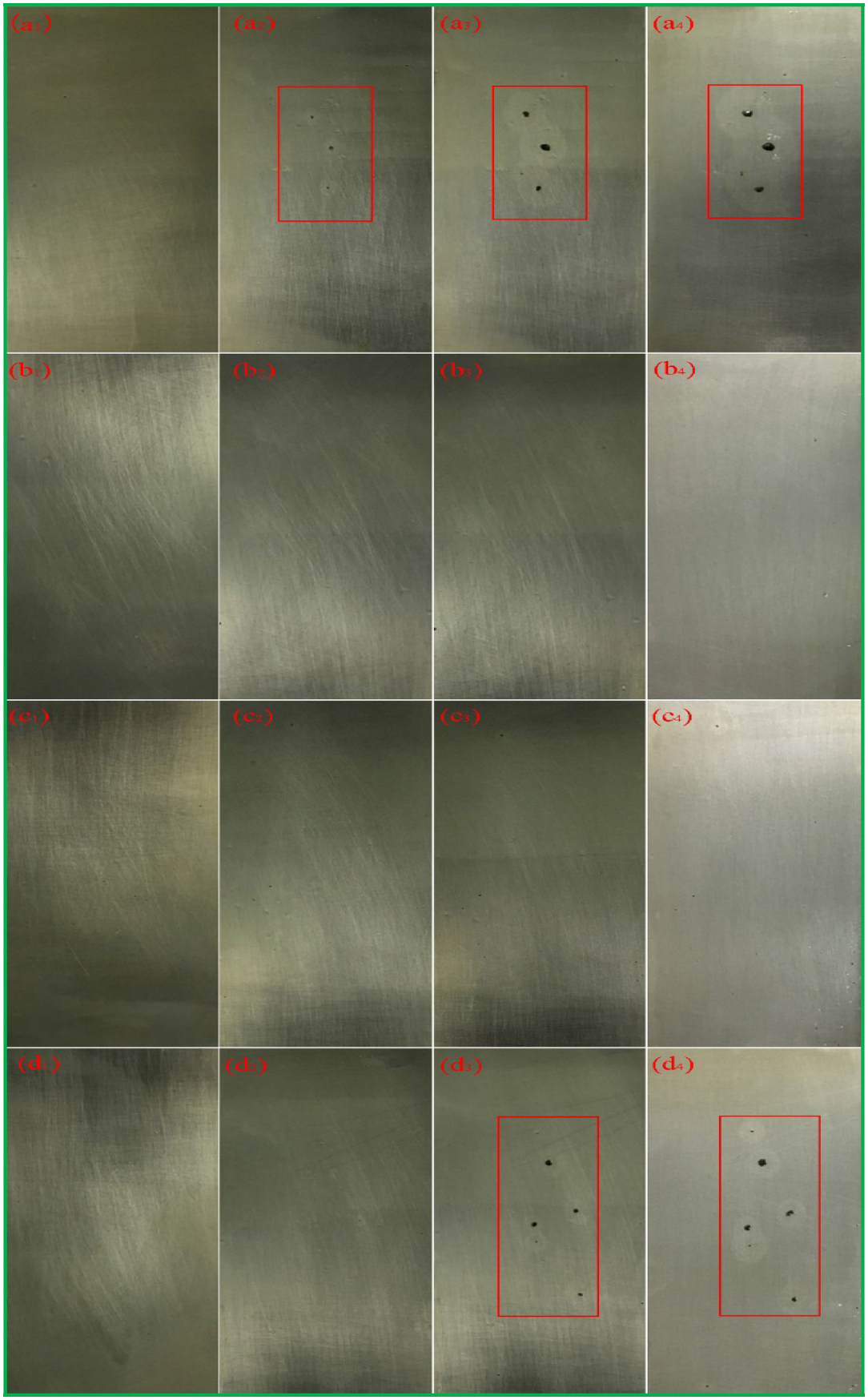

Fig. 12. Digital images of (a) neat epoxy coating, (b) EEUG/epoxy composite coating with 0.5 wt%, (c) EEUG/epoxy composite coating with 1 wt%, and (d) EEUG/epoxy composite coating with 2 wt% after (a_1, b_1, c_1, d_1) 0 h, (a_2, b_2, c_2, d_2) 100 h, (a_3, b_3, c_3, d_3) 200 h, and (a_4, b_4, c_4, d_4) 300 h neutral salt spray measurements.

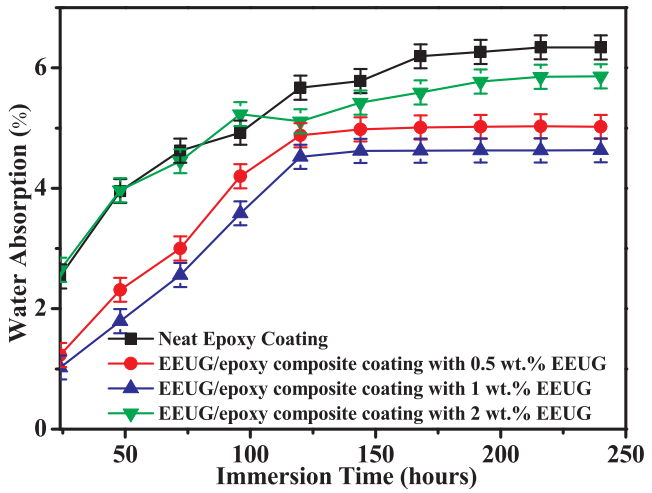

Fig. 13. Water absorption of immersed neat epoxy coating, EEUG/epoxy composite coating with 0.5 wt%, EEUG/epoxy composite coating with 1 wt%, and EEUG/epoxy composite coating with 2 wt%.

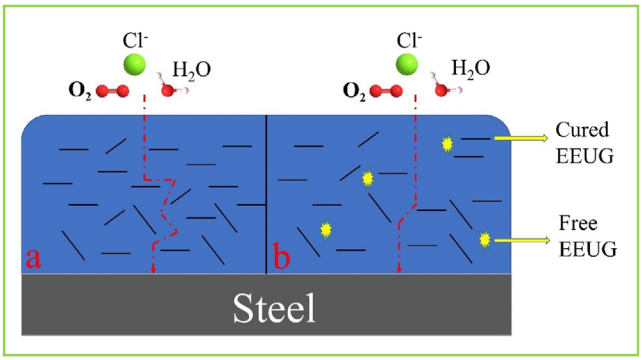

Fig. 14. Proposed mechanism of the enhanced corrosion protection of the EEUG/epoxy composite coating. (a) EEUG/epoxy composite coatings with 0.5 or 1 wt%; (b) the EEUG/epoxy composite coating with 2 wt%.

$3.321 \times 10^8\,\Omega\,cm^2$ and $8.846 \times 10^8\,\Omega\,cm^2$, respectively. Thereby, these as-obtained results suggest that the protective performances of the EEUG/epoxy composite coating with 0.5 and 1 wt% are remarkable improvement. Meanwhile, compared to the EEUG/epoxy composite coating with 0.5 wt%, the corrosion protection of the EEUG/epoxy composite coating with 1 wt% is further enhanced.

Additionally, the changes of Q_c for the coatings can reflect the above-mentioned conclusion. Generally, the penetration of the electrolyte solution in the coating often causes an increase in Q_c. As summarized in Table 2, the Q_c values for the EEUG/epoxy composite coating with 2 wt% and the neat epoxy coating are around $2.497 \times 10^{-5}\,\Omega^{-1}cm^{-2}S^n$ and $7.801 \times 10^{-4}\,\Omega^{-1}cm^{-2}S^n$ after 15 days of immersion, respectively, being at least four orders of magnitude larger than the EEUG/epoxy composite coating with 0.5 and 1 wt%. These results that there are only a small amount of electrolytes absorbed in the EEUG/epoxy composite coating with 0.5 and 1 wt%.

3.6. Neutral salt spray (NSS) measurement

To further understand the corrosion protection performance of the coatings, the neutral salt spray (NSS) tests were performed. It is well-known that the NSS test has been widely used to the corrosion protective property of the coating in the industry. The visual performance of the species subjected to the NSS test after 300 h is presented in Fig. 12. It is easily found that after 100 h NSS tests, the neat epoxy coating has the visibly localized pitting corrosions (Fig. 12a2), indicating the metal substrate has been seriously corroded. In the case of the EEUG/epoxy composite coating with 2 wt%, a number of obvious pitting corrosions have appeared after 300 h NSS tests (Fig. 12d3). After the incorporation of the 0.5 wt% and 1 wt% EEUG into the coating, respectively, the number of rust pots can be ignored during the entire NSS tests process (Fig. 12b and c). These demonstrate that the corrosion protective performance of the EEUG/epoxy composite coatings with 0.5 wt% and 1 wt% has been significantly improved.

3.7. Moisture absorption

To demonstrate the physical barrier ability of the EEUG/epoxy composite coatings and epoxy coatings for the H_2O molecules, the moisture adsorption measurements were carried out. After 350 h of the immersion times in the deionized water, the saturation was obtained for all epoxy coatings. Fig. 13 displays the water absorption of the EEUG/epoxy composite coating and epoxy coating. The water absorption for the coating was determined according to ASTM D570. The samples were removed from the water at regular intervals and weighed. The percentage gain (M_t) was calculated by the following equation:

$$M_t = \frac{W_{wet} - W_{dry}}{W_{dry}} \times 100\%$$

where W_{wet} and W_{dry} are the weight of the specimen after and before the immersion. As shown in Fig. 13, the water adsorption of the EEUG/epoxy composite coatings with 0.5 wt% and 1 wt% at saturation is much lower than that of the EEUG/epoxy composite coatings with 2 wt% and the neat epoxy coating. This indicates that the EEUG/epoxy composite coatings with 0.5 wt% and 1 wt% have good physical barrier performance for the H_2O molecules, reducing the penetration and absorption of water in the composite coatings. This can further explain that why the corrosion protection properties of the EEUG/epoxy composite coatings with 0.5 wt% and 1 wt% are much better than the EEUG/epoxy composite coating with 2 wt% and neat epoxy coating.

3.8. Reasonable corrosion protection mechanism

According to the above-obtained results, it is reasonably concluded that compared to the neat epoxy coating, the corrosion protection properties of the EEUG/epoxy composite coatings with 0.5 and 1 wt% have been remarkably enhanced. A reasonable explanation for this phenomenon is that the EEUG has the active epoxy groups, which can react with the polyamide hardener during the curing process, not only resulting in the formation of the closer three-dimensional cross-linked structures, but also causing the good dispersion in the composite coatings. Meanwhile, EEUG is easier to entangle with the epoxy resin due to the large relative molecular mass and the long molecular chain during the rapid evaporation of solvents process. Based on the two reasons, the EEUG/epoxy composite coatings have the much richer crosslinking densities. The much richer crosslinking densities act as the better physical barriers to prevent the electrolytes from passing through the coatings as illustrated in Fig. 14a. Therefore, the EEUG/epoxy composite coatings with 0.5 and 1 wt% exhibit the significant enhancement of corrosion resistance. However, when the doped EEUG is up to 2 wt% in the composite coatings, there is the existence of free EEUG in the coatings (Figs. 3d and 4d). These free EEUG can further form the large particles due to the agglomeration, leading to an increase of the molecular chain gap, which is beneficial for the formation of the diffusion channels for the electrolytes. This can promote the corrosive medium to pass through the coatings as illustrated in Fig. 14b. Thereby, the reasons can accounted for why the poor corrosion protection for the EEUG/epoxy composite coating with 2 wt%.

4. Conclusion

Epoxidized biomass eucommia gum (EEUG) was successfully prepared through a simple and green interface reaction. As a nanofiller, EEUG/epoxy composite coating with the contents up to 1 wt% can be easily processed. The epoxy group in the EEUG could react with the hardener, not only resulting in the good compatibility with epoxy resin in the composite coating, preventing the EEUG from agglomeration, but also leading to the formation of the much richer crosslinking densities, which is favor to increase the tensile strength. Furthermore, because of the richer crosslinking densities, the EEUG/epoxy composite coating containing 1 wt% EEUG shows the significantly enhanced corrosion protection performance. After 30 days immersed in 3.5 wt% NaCl solution, the R_f value still stabilized at about $8.846 \times 10^8\ \Omega\,cm^2$. It is believed that this facile process can be easily scaled up to generate epoxy composites with the biomass eucommia gum.

Acknowledgments

The research is financially supported by the National Natural Science Foundation of China (No. 51871097), the National Natural Science Foundation of Hunan Province, China (No. 2019JJ40033), the Research Foundation of Education Bureau of Guizhou Province, China (Guizhou [2015]402), the Joint Foundation of Science and Technology Department of Guizhou Province, China (Guizhou "LH" [2014]7430), and the Major Special Foundation of Research and Innovation of Qiannan Normal University for Nationalities, China (QNSY2018XK005).

Appendix A. Supplementary data

Supplementary data to this article can be found online at https://doi.org/10.1016/j.cej.2019.122323.

References

[1] M. Dehdab, Z. Yavari, M. Darijani, A. Bargahi, The inhibition of carbon-steel corrosion in seawater by streptomycin and tetracycline antibiotics: an experimental and theoretical study, Desalination 400 (2016) 7–17.
[2] J. Bhandari, F. Khan, R. Abbassi, V. Garaniya, R. Ojeda, Modelling of pitting corrosion in marine and offshore steel structures – A technical review, J. Loss Prev. Process Ind. 37 (2015) 39–62.
[3] G.M. Olmez, F.B. Dilek, T. Karanfil, U. Yetis, The environmental impacts of iron and steel industry: a life cycle assessment study, J. Cleaner Prod. 130 (2016) 195–201.
[4] Y. Zou, J. Wang, Y.Y. Zheng, Electrochemical techniques for determining corrosion rate of rusted steel in seawater, Corros. Sci. 53 (2011) 208–216.
[5] R.E. Melchers, Long-term corrosion of cast irons and steel in marine and atmospheric environments, Corros. Sci. 68 (2013) 186–194.
[6] X. Luo, X. Pan, S. Yuan, S. Du, C. Zhang, Y. Liu, Corrosion inhibition of mild steel in simulated seawater solution by a green eco-friendly mixture of glucomannan (GL) and bisquaternary ammonium salt (BQAS), Corros. Sci. 125 (2017) 139–151.
[7] B. Zhang, J. Li, X. Zhao, X. Hu, L. Yang, N. Wang, Y. Li, B. Hou, Biomimetic one step fabrication of manganese stearate superhydrophobic surface as an efficient barrier against marine corrosion and Chlorella vulgaris-induced biofouling, Chem. Eng. J. 306 (2016) 441–451.
[8] B. Qian, B. Hou, M. Zheng, The inhibition effect of tannic acid on mild steel corrosion in seawater wet/dry cyclic conditions, Corros. Sci. 72 (2013) 1–9.
[9] K. Lin, X. Luo, X. Pan, C. Zhang, Y. Liu, Enhanced corrosion resistance of LiAl-layered double hydroxide (LDH) coating modified with a Schiff base salt on aluminum alloy by one step in-situ synthesis at low temperature, Appl. Surf. Sci. 463 (2019) 1085–1096.
[10] A. Popova, M. Christov, A. Vasilev, Mono- and dicationic benzothiazolic quaternary ammonium bromides as mild steel corrosion inhibitors. Part III: influence of the temperature on the inhibition process, Corros. Sci. 94 (2015) 70–78.
[11] C. Verma, E.E. Ebenso, I. Bahadur, I.B. Obot, M.A. Quraishi, 5-(Phenylthio)-3H-pyrrole-4-carbonitriles as effective corrosion inhibitors for mild steel in 1M HCl: experimental and theoretical investigation, J. Mol. Liq. 212 (2015) 209–218.
[12] N.W. Pu, G.N. Shi, Y.M. Liu, X. Sun, J.K. Chang, C.L. Sun, M.D. Ger, C.Y. Chen, P.C. Wang, Y.Y. Peng, C.H. Wu, S. Lawes, Graphene grown on stainless steel as a high-performance and ecofriendly anti-corrosion coating for polymer electrolyte membrane fuel cell bipolar plates, J. Power Sources 282 (2015) 248–256.
[13] R.B. Figueira, C.J.R. Silva, E.V. Pereira, Organic–inorganic hybrid sol–gel coatings for metal corrosion protection: a review of recent progress, J. Coat. Technol. Res. 12 (2014) 1–35.
[14] C. Zhang, X. Luo, X. Pan, L. Liao, X. Wu, Y. Liu, Self-healing Li-Al layered double hydroxide conversion coating modified with aspartic acid for 6N01 Al alloy, Appl. Surf. Sci. 394 (2017) 275–281.
[15] M. Cui, S. Ren, S. Qin, Q. Xue, H. Zhao, L. Wang, Processable poly(2-butylaniline)/hexagonal boron nitride nanohybrids for synergetic anticorrosive reinforcement of epoxy coating, Corros. Sci. 131 (2018) 187–198.
[16] H. Gu, C. Ma, J. Gu, J. Guo, X. Yan, J. Huang, Q. Zhang, Z. Guo, An overview of multifunctional epoxy nanocomposites, J. Mater. Chem. C 4 (2016) 5890–5906.
[17] J. Gu, X. Yang, Z. Lv, N. Li, C. Liang, Q. Zhang, Functionalized graphite nanoplatelets/epoxy resin nanocomposites with high thermal conductivity, Int. J. Heat Mass Transf. 92 (2016) 15–22.
[18] F. Khelifa, Y. Habibi, L. Bonnaud, P. Dubois, Epoxy monomers cured by high cellulosic nanocrystal loading, ACS Appl. Mater. Interfaces 8 (2016) 10535–10544.
[19] Z.B. Shao, M.X. Zhang, Y. Li, Y. Han, L. Ren, C. Deng, A novel multi-functional polymeric curing agent: synthesis, characterization, and its epoxy resin with simultaneous excellent flame retardance and transparency, Chem. Eng. J. 345 (2018) 471–482.
[20] Y.Q. Shi, T. Fu, Y.J. Xu, D.F. Li, X.L. Wang, Y.Z. Wang, Novel phosphorus-containing halogen-free ionic liquid toward fire safety epoxy resin with well-balanced comprehensive performance, Chem. Eng. J. 354 (2018) 208–219.
[21] N. Domun, H. Hadavinia, T. Zhang, T. Sainsbury, G.H. Liaghat, S. Vahid, Improving the fracture toughness and the strength of epoxy using nanomaterials–a review of the current status, Nanoscale 7 (2015) 10294–10329.
[22] M.G. Hosseini, K. Aboutalebi, Improving the anticorrosive performance of epoxy coatings by embedding various percentages of unmodified and imidazole modified CeO 2 nanoparticles, Prog. Org. Coat. 122 (2018) 56–63.
[23] W. Li, H. Tian, B. Hou, Corrosion performance of epoxy coatings modified by nanoparticulate SiO2, Mater. Corros. 63 (2012) 44–53.
[24] B. Qian, J. Ren, Z. Song, Y. Zhou, One pot graphene-based nanocontainers as effective anticorrosion agents in epoxy-based coatings, J. Mater. Sci. 53 (2018) 14204–14216.
[25] M.A. El-Fattah, A.M. El Saeed, M.M. Dardir, M.A. El-Sockary, Studying the effect of organo-modified nanoclay loading on the thermal stability, flame retardant, anti-corrosive and mechanical properties of polyurethane nanocomposite for surface coating, Prog. Org. Coat. 89 (2015) 212–219.
[26] E. Husain, T.N. Narayanan, J.J. Taha-Tijerina, S. Vinod, R. Vajtai, P.M. Ajayan, Marine corrosion protective coatings of hexagonal boron nitride thin films on stainless steel, ACS Appl. Mater. Interfaces 5 (2013) 4129–4135.
[27] S.K. Dhoke, A.S. Khanna, Electrochemical impedance spectroscopy (EIS) study of nano-alumina modified alkyd based waterborne coatings, Prog. Org. Coat. 74 (2012) 92–99.
[28] A. Kalendová, D. Veselý, M. Kohl, J. Stejskal, Anticorrosion efficiency of zinc-filled epoxy coatings containing conducting polymers and pigments, Prog. Org. Coat. 78 (2015) 1–20.
[29] Y. Li, Z. Yang, H. Qiu, Y. Dai, Q. Zheng, J. Li, J. Yang, Self-aligned graphene as anticorrosive barrier in waterborne polyurethane composite coatings, J. Mater. Chem. A 2 (2014) 14139–14145.
[30] C.H. Chang, T.C. Huang, C.W. Peng, T.C. Yeh, H.I. Lu, W.I. Hung, C.J. Weng, T.I. Yang, J.M. Yeh, Novel anticorrosion coatings prepared from polyaniline/graphene composites, Carbon 50 (2012) 5044–5051.
[31] L. Gu, S. Liu, H. Zhao, H. Yu, Facile preparation of water-dispersible graphene sheets stabilized by carboxylated oligoanilines and their anticorrosion coatings, ACS Appl. Mater. Interfaces 7 (2015) 17641–17648.
[32] Y.H. Yu, Y.Y. Lin, C.H. Lin, C.C. Chan, Y.C. Huang, High-performance polystyrene/graphene-based nanocomposites with excellent anti-corrosion properties, Polym. Chem. 5 (2014) 535–550.
[33] B. Ramezanzadeh, S. Niroumandrad, A. Ahmadi, M. Mahdavian, M.H.M. Moghadam, Enhancement of barrier and corrosion protection performance of an epoxy coating through wet transfer of amino functionalized graphene oxide, Corros. Sci. 103 (2016) 283–304.
[34] S. Bohm, Graphene against corrosion, Nat. Nanotechnol. 9 (2014) 741–742.
[35] M. Zhu, Z. Du, Z. Yin, W. Zhou, Z. Liu, S.H. Tsang, E.H. Teo, Low-temperature in situ growth of graphene on metallic substrates and its application in anticorrosion, ACS Appl. Mater. Interfaces 8 (2016) 502–510.
[36] K.C. Chang, M.H. Hsu, H.I. Lu, M.C. Lai, P.J. Liu, C.H. Hsu, W.F. Ji, T.L. Chuang, Y. Wei, J.M. Yeh, W.R. Liu, Room-temperature cured hydrophobic epoxy/graphene composites as corrosion inhibitor for cold-rolled steel, Carbon 66 (2014) 144–153.
[37] C. Chen, S. Qiu, M. Cui, S. Qin, G. Yan, H. Zhao, L. Wang, Q. Xue, Achieving high performance corrosion and wear resistant epoxy coatings via incorporation of noncovalent functionalized graphene, Carbon 114 (2017) 356–366.
[38] W. Ren, H.M. Cheng, The global growth of graphene, Nat. Nanotechnol. 9 (2014) 726–730.
[39] C. Cui, A.T.O. Lim, J. Huang, A cautionary note on graphene anti-corrosion coatings, Nat. Nanotechnol. 12 (2017) 834–835.
[40] F. Zhou, Z. Li, G.J. Shenoy, L. Li, H. Liu, Enhanced room-temperature corrosion of copper in the presence of graphene, ACS Nano 7 (2013) 5939–6947.
[41] M. Schriver, W. Regan, W.J. Gannett, A.M. Zaniewski, M.F. Crommie, A. Zettl, Graphene as a long-term metal oxidation barrier-worse than nothing, ACS Nano 7 (2013) 5763–5768.
[42] W. Sun, L. Wang, T. Wu, M. Wang, Z. Yang, Y. Pan, G. Liu, Inhibiting the corrosion-promotion activity of graphene, Chem. Mater. 27 (2015) 2367–2373.
[43] W. Sun, L. Wang, T. Wu, Y. Pan, G. Liu, Inhibited corrosion-promotion activity of graphene encapsulated in nanosized silicon oxide, J. Mater. Chem. A 3 (2015) 16843–16848.
[44] H. Yahyaei, M. Ebrahimi, H.V. Tahami, E.R. Mafi, E. Akbarinezhad, Toughening mechanisms of rubber modified thin film epoxy resins: Part 2—Study of abrasion, thermal and corrosion resistance, Prog. Org. Coat. 113 (2017) 136–142.

[45] H. Yahyaie, M. Ebrahimi, H.V. Tahami, E.R. Mafi, Toughening mechanisms of rubber modified thin film epoxy resins, Prog. Org. Coat. 76 (2013) 286–292.
[46] D. Ratna, A.K. Banthia, Rubber toughened epoxy, Macromol. Res. 12 (2004) 12–21.
[47] Y. Sun, F. Liang, X. Qu, Q. Wang, Z. Yang, Robust reactive janus composite particles of snowman shape, Macromolecules 48 (2015) 2715–2722.
[48] W. Xu, J. Chen, S. Chen, Q. Chen, J. Lin, H. Liu, Study on the compatibilizing effect of janus particles on liquid isoprene rubber/epoxy resin composite materials, Ind. Eng. Chem. Res. 56 (2017) 14060–14068.
[49] J. Zhang, Z. Xue, Study on under-water sound absorption properties of Eucommia ulmoides gum and its blends, Polym. Bull. 67 (2011) 511–525.
[50] T. Bamba, E. Fukusaki, Y. Nakazawa, A. Kobayashi, In-situ chemical analyses of trans-polyisoprene by histochemical staining and Fourier transform infrared microspectroscopy in a rubber-producing plant, Eucommia ulmoides Oliver, Planta 215 (2002) 934–939.
[51] Y. Nakazawa, T. Takeda, N. Suzuki, T. Hayashi, Y. Harada, T. Bamba, A. Kobayashi, Histochemical study of trans-polyisoprene accumulation by spectral confocal laser scanning microscopy and a specific dye showing fluorescence solvatochromism in the rubber-producing plant, E. ulmoides Oliver, Planta 238 (2013) 549–560.
[52] Y. Wang, L. Xia, Z. Xin, Triple shape memory effect of foamed natural Eucommia ulmoides gum/high-density polyethylene composites, Polym. Adv. Technol. 29 (2018) 190–197.
[53] Q. Sun, X. Zhao, D. Wang, J. Dong, D. She, P. Peng, Preparation and characterization of nanocrystalline cellulose/Eucommia ulmoides gum nanocomposite film, Carbohydr. Polym. 181 (2018) 825–832.
[54] X. Luo, J. Zhong, Q. Zhou, S. Du, S. Yuan, Y. Liu, Cationic reduced graphene oxide as self-aligned nanofiller in the epoxy nanocomposite coating with excellent anticorrosive performance and its high antibacterial activity, ACS Appl. Mater. Interfaces 10 (2018) 18400–18415.
[55] F. Lei, C. Zhang, Z. Cai, J. Yang, H. Sun, D. Sun, Epoxy toughening with graphite fluoride: toward high toughness and strength, Polymer 150 (2018) 44–51.
[56] S. Du, Y. Wang, C. Zhang, X. Deng, X. Luo, Y. Fu, Y. Liu, Self-antibacterial UV-curable waterborne polyurethane with pendant amine and modified by guanidinoacetic acid, J. Mater. Sci. 53 (2017) 215–229.
[57] A.B. Chaudhari, P.D. Tatiya, R.K. Hedaoo, R.D. Kulkarni, V.V. Gite, Polyurethane prepared from neem oil polyesteramides for self-healing anticorrosive coatings, Ind. Eng. Chem. Res. 52 (2013) 10189–10197.
[58] F. Yang, Q. Liu, X. Li, L. Yao, Q. Fang, Epoxidation of eucommia ulmoides gum by emulsion process and the performance of its vulcanizates, Polym. Bull. 74 (2017) 3657–3672.
[59] L. Xia, Y. Wang, Z. Ma, A. Du, G. Qiu, Z. Xin, Preparation of epoxidized Eucommia ulmoides gum and its application in styrene-butadiene rubber (SBR)/silica composites, Polym. Adv. Technol. 28 (2017) 94–101.
[60] B.U. Kang, J.Y. Kim, J. Kim, S.S. Lee, M. Park, S. Lim, C.R. Choe, Effect of molecular weight between crosslinks on the fracture behavior of rubber-toughened epoxy adhesives, J. Appl. Polym. Sci. 79 (2001) 38–48.
[61] B.J. Rohde, K.M. Le, R. Krishnamoorti, M.L. Robertson, Thermoset blends of an epoxy resin and polydicyclopentadiene, Macromolecules 49 (2016) 8960–8970.
[62] V. Nigam, D.K. Setua, G.N. Mathur, Failure analysis of rubber toughened epoxy resin, J, Appl. Polym. Sci. 87 (2002) 861–868.
[63] X. Xiong, L. Zhou, R. Ren, S. Liu, P. Chen, The thermal decomposition behavior and kinetics of epoxy resins cured with a novel phthalide-containing aromatic diamine, Polym. Test. 68 (2018) 46–52.
[64] I.H. Kwon, W.H. Jo, The equation of state theory for glass transition temperature in miscible polymer blends, Polym. J. 24 (1992) 625–632.
[65] Y. Feng, Y.F. Cheng, An intelligent coating doped with inhibitor-encapsulated nanocontainers for corrosion protection of pipeline steel, Chem. Eng. J. 315 (2017) 537–551.